Journal of Applied Polymer Science

Thermomechanical Properties of Alkali Treated Jute-Polyester/ Nanoclay Biocomposites Fabricated by VARTM Process

Mohammad Washim Dewan,[1] Mohammad Kamal Hossain,[1] Mahesh Hosur,[2] Shaik Jeelani[2]
[1]Mechanical Engineering Department, Tuskegee University, Tuskegee, Alabama 36088
[2]Materials Science and Engineering Department, Tuskegee University, Tuskegee, Alabama 36088
Correspondence to: M. K. Hossain (E-mail: hossainm@mytu.tuskegee.edu)

ABSTRACT: A systematic study was carried out to investigate the effect of alkali treatment and nanoclay on thermomechanical properties of jute fabric reinforced polyester composites (JPC) fabricated by the vacuum-assisted resin transfer molding (VARTM) process. Using mechanical mixing and sonication process, 1% and 2% by weight montmorillonite K10 nanoclay were dispersed into B-440 premium polyester resin to fabricate jute fabric reinforced polyester nanocomposites. The average fiber volume was determined to be around 40% and void fraction was reduced due to the surface treatment as well as nanoclay infusion in these biocomposites. Dynamic mechanical analysis (DMA) revealed enhancement of dynamic elastic/plastic responses and glass transition temperature (T_g) in treated jute polyester composites (TJPC) and nanoclay infused TJPC compared with those of untreated jute polyester composites (UTJPC). Alkali treatment and nanoclay infusion also resulted in enhancement of mechanical properties of JPC. The maximum flexural, compression, and interlaminar shear strength (ILSS) properties were found in the 1 wt % nanoclay infused TJPC. Fourier transform-infrared spectroscopy (FT-IR) revealed strong interaction between the organoclay and polyester that resulted in enhanced thermomechanical properties in the composites. Lower water absorption was also observed due to surface treatment and nanoclay infusion in the TJPC. © 2012 Wiley Periodicals, Inc. J. Appl. Polym. Sci. 128: 4110–4123, 2013

KEYWORDS: biomaterials; composites; crosslinking; mechanical properties; thermal properties

Received 7 May 2012; accepted 22 September 2012; published online 17 October 2012
DOI: 10.1002/app.38641

INTRODUCTION

Composite materials made from synthetic fibers such as glass fiber and carbon fibers are already available for consumer and industrial uses. Manufacturing of synthetic fiber composites not only consume huge energy but also their disposal at the end of the life cycle is very difficult since there is virtually no recycling option. Stringent environmental legislation and consumer awareness have forced industries to develop new technology based on renewable feedstock that are independent of fossil fuels. Industrial crops grown for fiber have the potential to supply enough renewable biomass for various bio-products including composites. The scope of possible uses of natural fibers is enormous.[1] Natural fiber reinforced composites are light weight and possess good thermal and acoustic insulating properties, higher specific properties, and higher resistance to fracture.[2–4] Lignocellulosic biofibers derived from various sources such as leaf, bast, fruit, grass, or cane contribute to the strength and stiffness of bio as well as synthetic polymer composites in various applications.[5] Jute fiber is known to have excellent tensile strength and a high modulus among lignocellulosic fibers.[6] Different types of surface treatment procedures have been suggested to enhance the interaction between natural fiber and matrix. Alkali treatment is the easiest and most widely investigated surface treatment technique for natural fibers. The effect of alkali treatment on mechanical and thermal properties of composites has been studied by many researchers.[7–9] They found a better adhesion of fibers with matrices due to the surface modification by alkali treatment.

Nanoscale materials offer the opportunity to explore new behavior beyond those established in conventional materials. Various types of nanoparticles, including carbon nanofiber, carbon nanotube, nanoclay, and metal oxides have been used to improve the performance of composites. It has been established that the addition of a small amount of nanoparticle into a matrix can improve thermal and mechanical properties significantly without compromising the weight or processability of the composite.[10] For example, it has been observed that moisture barrier, flame resistance, thermal, and mechanical properties of polymeric composites can be improved by adding a small amount of nanoclay as filler particles.[11] The higher surface area

is one of the most promising characteristics of nanoparticles due to their ability in creating good bonding in composites. The dispersion of nanoparticles in the matrix is one of the most important parameters in fabricating nanophased composites. It highly depends on processing techniques such as solution blending, shear mixing, *in situ* polymerization, ultrasonic cavitation, and high pressure mixing.[12–14]

Many researchers have used montmorillonite nanoclay as filler in polymeric composites and their laminates for its low cost, availability, well-known intercalation/exfoliation chemistry, high surface area, and high surface reactivity. The montmorillonite layer aspect ratio can be as high as 1000 in the well dispersed state without breaking of layers. Its surface area is in the range of 220 to 270 m^2/g. Additionally, nanoclay has excellent physical and thermal properties. Nanoclay reinforced polymer composites and their laminates have excellent characteristics, including improved physical (dielectric, optical, permeability, and shrinkage), thermal (flammability, decomposition, coefficient of thermal expansion, and thermal stability), and mechanical (toughness, strength, and modulus) properties even at a very low filler loading. Generally montmorillonite clay is hydrophilic in nature. The incompatibility of hydrophilic clay layers with hydrophobic polymer chains makes the dispersion of clay within polymer matrix difficult and leads to weak interfacial interactions. Nanoclays are miscibile only with a few hydrophilic polymers such as poly(ethylene oxide) and poly(vinyl alcohol).[15,16] In order to achieve an enhanced compatibility to various polymer matrices, the clay surface is organically treated to make them compatible with polymers by assisting in intergallery absorption. This modification is done by ion-exchange utilizing suitable organic surfactants, including primary, secondary, tertiary, and quaternary alkylammonium or alkylphosphonium cations. The most widely used surfactant in polymer clay nanocomposite processing is quaternary ammonium salts due to their high ion exchange efficiency. This organic surfactant can significantly lower the surface energy of the clay layers and match their surface polarity with polymer polarity. Hence, polymer chains can be more easily wetted on the layer surface generating a larger interlayer distance. This larger interlayer distance will facilitate the nanoclay intercalated and/or exfoliated into the polymeric matrix that will result in enhanced properties in the composite. Thus, the reinforced properties largely depend on the degree of dispersion of silicate platelets within a polymer matrix, which is a function of polymer-nanoclay compatibility. Basically, the degree of interaction between the surfactant monomer and polymer is crucial to achieve nanoscale dispersion of clay layers to obtain the ultimate properties of nanocomposites. Hence, organically modified montmorillonite clay is used in this study. Incorporating a small amount of nanoclay can improve composite properties significantly. However, higher clay loading above a certain threshold value increases the viscosity of the matrix. A higher clay loading also increases the amount of air bubble during the mixing process. Therefore, an optimum amount of nanoclay will provide better properties as it is uniformly dispersed into the composite.

Jute fibers and polyester resins are low-cost materials for fabricating biocomposites. Several researchers worked on jute polyester composites produced by various processing methods.[17–21] Alkali-treated jute roving polyester composites exhibited better mechanical properties due to better fiber-matrix mechanical interlocking at the interface.[22] Higher storage modulus and thermal transition temperatures have been found in surface treated jute/polyester composites processed by hand lay-up.[18] Jiang et al. also found improvement in storage modulus in 5 wt % cellulose nanowhisker infused biopol composites prepared by solution casting and extrusion followed by injection molding process.[23] Flexure strength, flexure modulus, and interlaminar shear strength were improved by 20%, 23%, and 19%, respectively, in the 4-h alkali-treated 35% jute fiber reinforced vinyl ester composites compared with those of untreated ones.[24] Jute fabric reinforced polyester composites produced by hand lay-up technique showed maximum compression strength, compression modulus, and interlaminar shear strength (ILSS) to be 45 MPa, 2.1 GPa, and 10 MPa, respectively, at a fiber volume fraction of 45%.[2] Hwang et al. showed 45% improvement in the ILSS of jute fiber reinforced polypropylene composites with 5% maleic anhydride coupler prepared by the compression molding process.[25] The ILSS of glass-epoxy composites manufactured by the VARTM process was improved by 31% due to the addition of 2% oxidized multiwalled carbon nanotubes.[26] Water absorption is a problem with composites, particularly with natural fiber reinforced composites. For example, synthetic fiber reinforced composites absorb water around up to 4% depending on type and amount of fiber, type and amount of resin, and environmental conditions[27,28] whereas water content of natural fiber reinforced composites varies between 5 and 15%.[29,30] For example, jute fiber reinforced polyester composites fabricated by the VARTM process exhibited 8.9% water gain at room temperature having fiber volume fraction of about 40%.[31] Vilay et al. fabricated alkali treated and untreated baggage fiber reinforced polyester composites using the vacuum bagging process. They reported that 7% and 12% water were absorbed by the treated and untreated fiber reinforced composites, respectively, under the same condition.[32] Any natural fiber reinforced composite to be effective needs to bring the water absorption rate down to 4% or below.

To the best of our knowledge, there is no study reported in the open literature on jute based polyester nanophased composite that was processed by the VARTM process. Hence, the objectives of this study are to fabricate nanoclay-infused untreated/alkali treated jute fiber reinforced polyester biocomposites using the VARTM process and explore their thermomechanical properties for structural applications. Using mechanical mixing and sonication process, montmorillonite K10 nanoclays were dispersed into B-440 premium polyester resin to fabricate jute fiber reinforced polyester nanocomposites. Nanoclay content was varied to observe its effect on the performance of jute fiber composites manufactured by the cost-effective VARTM process. Various percentage of nanoclay loadings (1–4 wt %) were tried. However, a higher percentage of nanoclay (above 2 wt %) results in considerable increase in the viscosity of the polyester resin that induces improper impregnation of the reinforcements. Moreover, a higher clay content causes agglomeration in the sonication mixing process that leads to easy material removal

compared to the lower clay content.[33–35] In addition, pot life of polyester resin is very short, usually 15 to 20 min. It was very difficult to infuse highly viscous resin within 15 to 20 min by the VARTM process. Hence, only 1 and 2 wt % nanoclay were infused in this study.

Common solvent method or solution based processing techniques could be employed to solve this problem. However, increase of clay content will require an increasing amount of solvent solution for proper dispersion. This will require a larger amount of energy to remove the solvent that may cause thermal degradation of the polyester.[35] It will also increase the fabrication cost and is not feasible for industry application due to the use of solvent. However, it is important to control the size of the clay agglomerates for obtaining a better dispersion of nanoclay in the VARTM process. Observations of the microstructures of the nanocomposites suggest that ultrasonic dispersion provides the best results in terms of size and dispersion.[36]

Jute fiber reinforced composites have been studied for a number of years. Researchers have found that composites having a fiber volume fraction of 30 to 40% provide optimum properties.[31,37,38] Hence, in this study, we have decided to maintain a similar fiber volume fraction in our composites. The thermomechanical performances of these composites were evaluated using DMA, flexure, interlaminar shear, and compression tests. The fracture morphology of the flexure and compression tested samples were analyzed using scanning electron microscope (SEM) and optical microscope (OM). Interaction between polyester and organoclay was studied by FT-IR. The effects of alkali treatment and nanoclay on the water absorption of the jute polyester composites were also evaluated in this study.

MATERIALS AND METHODS

Materials Selection

Commercially available B-440 premium polyester resin was purchased from U.S. Composites. Hessian jute fabrics (Natural Color Burlap, Material: 100% Jute, Width: 47", 11 Oz.) were supplied by OnlineFabricStore.net. Organically modified montmorillonite K10 nanoclay (surface area: 220–270 m^2/g, thickness of each layer: 1 nm and lateral dimension: several microns) was procured from Sigma-Aldrich. Ammonium based organic modifiers are generally used for the modification of montmorillonite nanoclay.[39] Polyester, jute, and nanoclay were used as matrix, reinforcement, and nanofillers, respectively because of their good property values and low cost. Polyester resin comes in two parts: part A (polyester resin) and part B (methyl ethyl ketone peroxide, MEKP). For alkali treatment of jute fibers, 5 wt % sodium hydroxide (NaOH) solution was used.

Alkali Treatment

Jute fibers were soaked with 5 wt % NaOH solution for 2 h at 30°C. Then the fibers were rinsed with water several times to remove NaOH and dissolved impurities. After rinsing, the fibers were dried in an oven at 100°C for 5 h. The alkaline treatment increases the surface roughness of natural fibers. It results in better mechanical interlocking properly. It also increases the amount of cellulose exposed on the fiber surface, thus increasing the number of possible reaction sites.[40] The alkali treatment further results in a large number of –OH groups accessible on the surface of fibers.[41] It breaks down fiber bundles into single fibers and increases effective surface area available for interacting with matrix.

Resin Preparation and Composites Fabrication

Polyester resin has two parts. For nanoclay infused specimens, desired amount of nanoclay was first mixed with part A of the resin by a high-speed mechanical stirrer for 5 min followed by sonication for 60 min in a beaker.[42] Sonication was performed using a high intensity ultrasonic irradiation (Ti-horn, 20 kHz Sonics Vibra Cell, Sonics Mandmaterials, Inc.). The mixing process was carried out in a pulse mode: 20 s on and 20 s off and the amplitude was 40% of the maximum value. The beaker was submerged in a continuously cooled water bath to maintain the temperature at 25°C during the sonication process. After sonication, the mixture was cooled in a water bath and degasified using a vacuum oven. Once the bubbles were completely removed from the mixture, 0.7 wt % initiator (MEKP) was added and stirred using a mechanical stirrer for about 2 to 3 min. The sample was further degasified to remove the bubbles produced during the initiator mixing. Composite panels were then fabricated using the vacuum-assisted resin transfer molding (VARTM) process. The mold was left for about 24 h at room temperature for curing the resin. After 24 h, the mold was opened and the panel was placed to an oven at 110°C for 3 h for post curing. After postcuring, test coupons were prepared according to the ASTM standard from different sections of the panels. Coupons were randomly collected for each type of test.

During infusion of nanoclay loaded resin into mold, there is always a possibility of filtering of nanoparticles by the top layers of the fabric. Filtration effect depends on the type of fiber, type and amount of nanofillers, and resin infusion techniques. This filtration effect generally occurs in nanoparticles infused composites fabricated by the VARTM process due to the filtering role of the fabrics.[26,36,43] Hence, small variations of nanoclay content are expected in top and bottom half of the composite panels.

Experimental Procedures

Void and Fiber Volume Fraction Calculation. Void content of the jute biopol composites was determined according to the ASTM D 2734-94 standard using composite mixing eqs. (1) through (4).

$$V_v\ (\%) = (\rho_t - \rho_e)/\rho_t \times 100 \quad (1)$$

$$\rho_t = 1/(W_f/\rho_f + W_m/\rho_m + W_n/\rho_n) \quad (2)$$

$$V_f = (W_f/\rho_f)/(W_f/\rho_f + W_m/\rho_m + W_n/\rho_n) \quad (3)$$

$$\rho_e = W_s/V_s \quad (4)$$

Here, V_v, V_f, ρ_t, and ρ_e are the void fraction, fiber volume fraction (considering no void), theoretical density, and experimental density of the composites, respectively. W_f, W_m, and W_n are the weight fractions and ρ_f, ρ_m, and ρ_n are the densities of fiber, matrix, and nanoclay, respectively. W_s and V_s are the weight (g) and volume (cm^3) of the specimens. Densities of polyester resin, jute fiber, and nanoclay were taken as 1.19 g/cm^3, 1.4 g/cm^3, and 2.35 g/cm^3, respectively. Experimental densities of composites were calculated using eq. (4). Three samples from each category were chosen to calculate composite experimental density. For void fraction calculation, average experimental density (ρ_e) was used.[44]

Table I. Density, Void Fraction, and Fiber Volume Fraction of JPC

	Theoretical density (ρ_t) (gm/cm^3)	Experimental density (ρ_e) (gm/cm^3)	Void fraction (%)	Fiber volume fraction (V_f)
UTJPC	1.288 ± 0.021	1.181 ± 0.075	8.33	0.449 ± 0.041
TJPC	1.271 ± 0.013	1.203 ± 0.049	5.38	0.385 ± 0.034
1% TJPC	1.272 ± 0.010	1.211 ± 0.051	4.75	0.389 ± 0.035
2% TJPC	1.287 ± 0.011	1.222 ± 0.070	5.075	0.416 ± 0.039

Thermogravimetric Analysis (TGA). To test the filtering effect, thermogravimetric analysis (TGA) tests were performed on randomly selected samples from top-half and bottom-half of the nanoclay-loaded composite panels. TGA was conducted with TA Instruments Q 500 setup fitted with nitrogen purge gas. Three samples from each category were tested. Samples were kept in a platinum sample pan, weighed, and heated to 700°C from room temperature at a heating rate of 5°C/min under nitrogen atmosphere. The real time characteristic curves were generated by a Universal Analysis-TA Instruments data acquisition system.

Dynamic Mechanical Analysis (DMA). Dynamic mechanical analysis of various jute polyester composites was carried out on TA instrument Q800 according to the ASTM D4065-01 standard.[45] Nominal specimen dimensions were 60 mm × 12 mm × 3 mm. The tests were run under a double cantilever beam mode with a frequency of 1 Hz and an amplitude of 15 μm. The temperature was ramped from 30°C to 180°C at a rate of 5°C/min. At least three samples from each category were tested to obtain the average dynamic elastic response (storage modulus), dynamic plastic response (loss modulus), and the ratio of loss modulus and storage modulus (tan δ).

Flexure Test. Flexural properties of jute-polyester composites with/without nanoclay were evaluated using a Zwick Roell testing unit under three point bending mode according to the ASTM D790-02 standard at a crosshead speed of 2.0 mm/min. Span length to thickness ratio of the specimen was 16 and the width of the specimen was 12 mm. Five samples from each category were tested to obtain the average result.

Interlaminar Shear Strength (ILSS) Test. The apparent interlaminar shear strength (ILSS) of the jute polyester composites was determined by the short beam shear (SBS) test. ILSS testing was carried out using a Zwick-Roell testing unit under three point bending mode according to the ASTM D 2344-00 standard at a crosshead speed of 1.3 mm/min. Span length to depth ratio of the specimen was 6 and the width of the specimen was double of the thickness. By using a short beam, it is assumed that the beam is short enough to minimize bending stresses resulting in an interlaminar shear failure by cracking along a horizontal plane between the laminae. The ILSS was calculated using the eq. (5).

$$\text{ILSS} = (0.75 \times P)/(b \times h) \quad (5)$$

where P is the breaking load (N), b and h are the width and thickness of the specimen, respectively, in mm. Three identical specimens from each category were tested and the average ILSS was calculated.

Quasi-Static Compression Test. Quasi-static compression tests of the jute polyester composites were performed using a servo-hydraulic MTS testing unit according to the ASTM D 695-02 standard at a cross head speed of 1.2 mm/min. The dimensions of the specimens were 12.5 mm × 12.5 mm × 5 mm and loaded in the fiber direction. The end friction between the specimen and the machine was minimized using a lubricant at the contact area. Contact surfaces were prepared parallel by grinding for the full contact and to eliminate potential bending moment. Five samples from each category were tested to obtain the average result.

Fracture Morphology Study. Morphology of fractured specimens was studied by JEOL JSM5800 scanning electron microscope (SEM) and Olympus DP72 optical microscope (OM).

Polyester-Organoclay Interaction Study by FT-IR. A Fourier transform-infrared (FT-IR) spectrophotometer was employed for the study of chemical reaction between nanoclay and polyester resin using Nicolet 6700 DX IR spectrophotometer with attenuated total reflectance (ATR) sampling. The crystal material for the ATR was diamond. The background was taken after every 60 min and each spectrum was recorded by co-adding 32 scans at 4 cm^{-1} resolution within the range 4000 to 600 cm^{-1}. Three samples from each category were selected randomly and tested. The background spectrum of KBr pellet was subtracted from the sample spectra.

Water Absorption Test. In order to measure the water absorption of jute polyester composites, five rectangular specimens from each category were prepared with dimensions of 80 mm × 13 mm × 3.5 mm. The specimens were dried in an oven at 105°C for 2 h, cooled in a desiccator, and immediately weighed (W_0). Samples weights were measured using a precision balance having an accuracy of 0.0001 g. The samples were then immersed into distilled water according to the ASTM D 570-99 standard for 24 h. After removing the samples, the excess water on the surface of the specimens was removed using clothes. The final weight (W) of the specimens was then taken. The water absorption (M_w) of the specimens was calculated using eq. (6).

$$M_w\ (\%) = (W - W_0)/(W_0) \times 100 \quad (6)$$

RESULTS AND DISCUSSIONS

Results

Void Fraction and Fiber Volume Fraction. When the fill and warp direction fiber cross each other, it allows voids to be formed in the composite system. The presence of trapped air or volatile materials and incomplete wetting out of the fibers by the matrix also causes the void in the fiber reinforced composites.[22,46] Theoretical density, experimental density, void

Applied Polymer SCIENCE

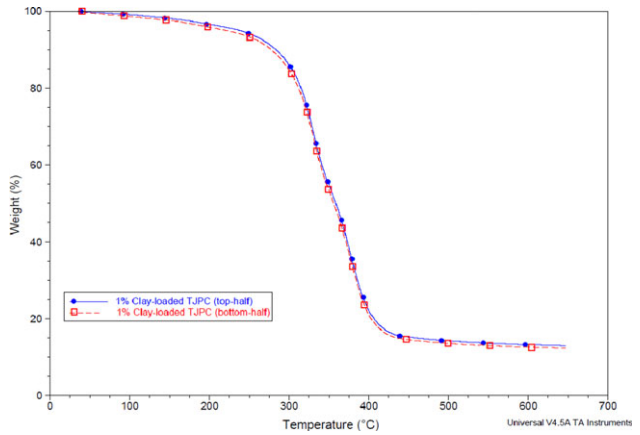

Figure 1. TGA curves to show the filtering effect in 1 wt % nanoclay-loaded TJPC. [Color figure can be viewed in the online issue, which is available at wileyonlinelibrary.com.]

fraction, and fiber volume are presented in Table I. A higher percentage of voids were found in the UTJPC compared with the TJPC. In this study, there was a small variation in fiber volume fraction due to limitations in the fabrication process. To compare the properties, the results were normalized by dividing experimentally acquired properties by the respective fiber volume fractions. Nanoclay infused treated jute fiber reinforced composites demonstrated same trend even after normalization.

Thermogravimetric Analysis (TGA) Test Results on Nanoclay Filtering Effect

To test the filtering effect in our study thermogravimetric analysis (TGA) tests were performed. First, six samples (70 mm × 12.5 mm × 3 mm) from 1% and 2 % TJPC panels (three in each category) were randomly selected. These samples were cut into halves along the thickness with a diamond cutter, yielding 12 top-half and bottom-half samples. Approximately 12 to 13 mg portions from these 12 samples were prepared for the TGA tests by using a diamond cutter and grinder. From the TGA analysis, it was observed that at about 650°C the ash residue from each sample reached an asymptotic value. The variation of ash content in top- and bottom-half of the 1 wt % nanoclay-loaded TJPC panel is presented in Figure 1. The average ash content for the 1% TJPC top-half samples was 0.21% higher than that from the 1% TJPC bottom-half samples. For the 2% TJPC, the ash content was found to be 0.56% higher for the top-half samples. Thus, these results lend support to our conjecture that the filtering effect is very low for the 1% TJPC and moderate for the 2% TJPC.

Dynamic Mechanical Analysis (DMA) Test Results. The variation in storage modulus of the jute polyester composite with surface treatment and nanoclay loading is shown in Figure 2(a) as a function of temperature. The results indicate the increase in the storage modulus at room temperature with surface treatment and nanoclay loading. TJPC samples with 2 wt.% nanoclay showed the highest storage modulus followed by 1% nanoclay infused and TJPC. TJPC, 1% and 2% nanoclay TJPC showed 16%, 18%, and 43% improvement in storage modulus, respectively, compared with UTJPC. In Figure 2(a), the sharp drop in storage modulus indicates the glass transition temperature (T_g) of the composites. The entire region can be divided into two sections: below T_g (glassy plateau region) and above T_g (rubbery plateau region). The operating temperature of the composite should be below T_g. The flatter section above T_g indicates the rubbery region of the composites. The storage

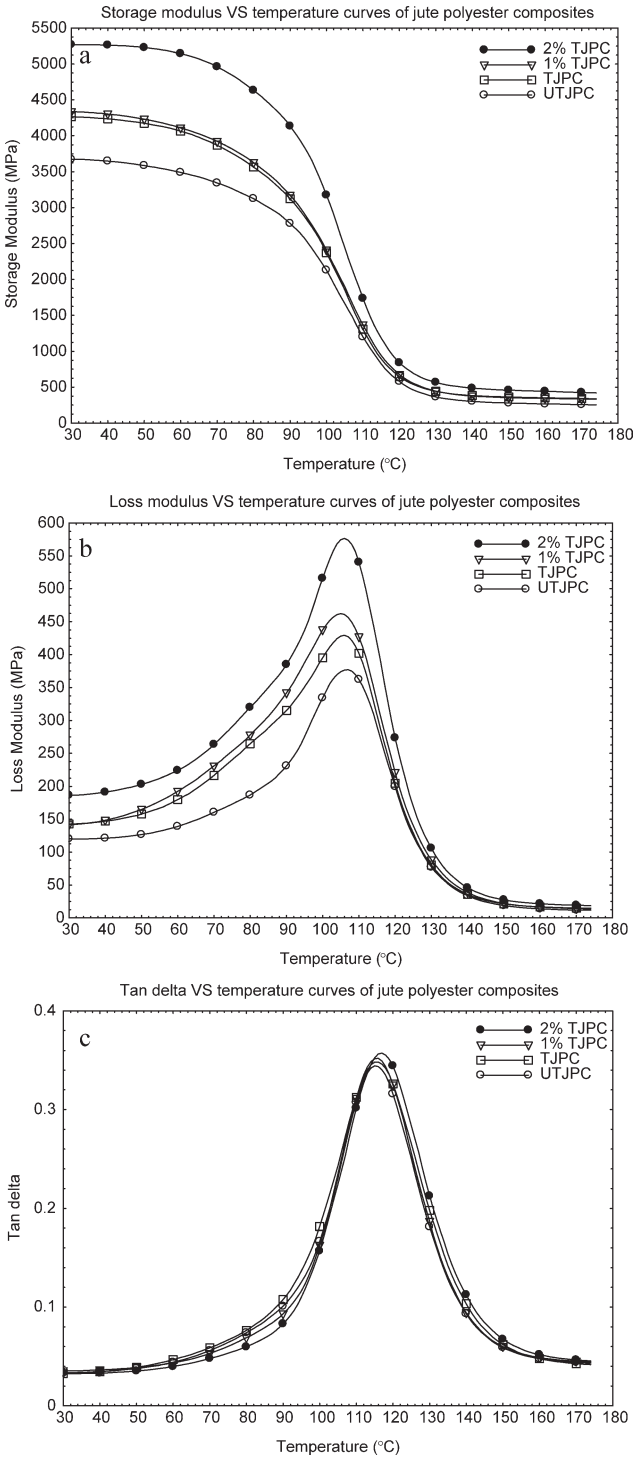

Figure 2. DMA curves of JPC (a) storage modulus, (b) loss modulus, and (c) tan delta (tan δ).

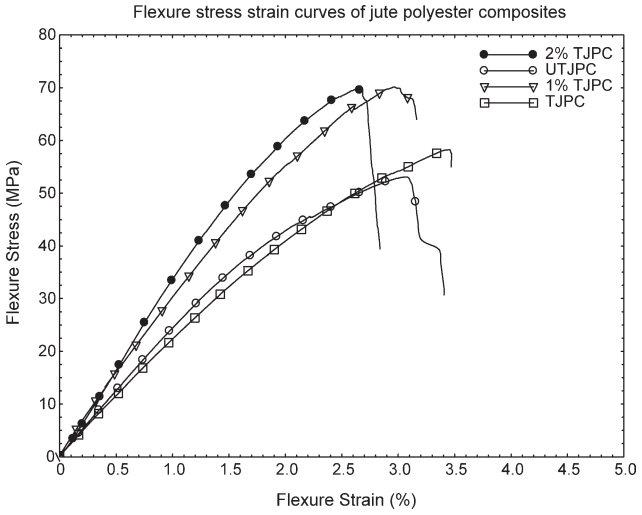

Figure 3. Flexure stress–strain curves of jute polyester composites.

modulus increased slightly with clay loading in the rubbery plateau region.

Figure 2(b) shows the variation of loss modulus of the jute polyester composites as a function of temperature. Loss modulus values increased with surface treated jute fibers and nanoclay loading. TJPC samples loaded with 2% nanoclay exhibited about 52% improvement in the loss modulus compared with UTJPC. The variation of tan δ with temperature is shown in Figure 2(c). The peak of the tan δ curve was used to measure the glass transition temperature of the composites. UTJPC and TJPC showed average T_g about 115°C and 116°C. Nanoclay infused TJPC (2 wt %) showed T_g about 3°C higher compared with UTJPC.

Flexural Test Results. Typical flexure stress–strain curves are shown in Figure 3. Variation in flexural strength, modulus, and strain at maximum stress with surface treatment of jute fiber and nanoclay are presented in Table II. The higher flexural strength was observed in the TJPC and nanoclay infused TJPC. TJPC showed about 15% improvement in the flexural strength compared to UTJPC. Nanoclay loaded TJPC (1 wt % and 2 wt %) showed 40% and 35% improvement in flexural strength, and 20% and 17% improvement in flexural modulus compared with those of UTJPC, respectively. Figure 4 shows SEM micrographs of the fracture surfaces of JPC after flexure tests. In case of UTJPC, matrix cracking and interfacial debonding occur for the weaker interfacial bonding between the fiber and matrix. No fiber breakage was observed in UTJPC.

The average experimental flexure strength of each category of samples ranged from a low of 49.59 ± 1.40 MPa for UTJPC to a high of 69.63 ± 0.46 MPa for 1 wt % nanoclay-loaded TJPC. The low and high values for the experimental flexure modulus are 4.87 ± 0.18 GPa for UTJPC and 5.86 ± 0.43 GPa for 1 wt % nanoclay-loaded TJPC. The corresponding low and high values for normalized flexure strength and normalized flexure modulus are 110.45 ± 3.12 MPa, 179.00 ± 1.18 MPa, 10.85 ± 0.40 GPa, and 15.06 ± 1.11 GPa, respectively (Table II). The analysis of variance (ANOVA)[47] was performed to analyze the

Table II. Flexure Test Results of Jute Polyester Composites

	Flexure strength (MPa)	Change in strength (%)	Strain at maximum stress (%)	Modulus (GPa)	Change in modulus (%)	Normalized strength (MPa/V_f)	Normalized modulus (GPa/V_f)	*P*-value from ANOVA test (strength)
UTJPC	49.59 ± 1.40	0	2.59 ± 0.10	4.87 ± 0.18	0	110.45 ± 3.12	10.85 ± 0.40	0.0001
TJPC	57.46 ± 1.73	15.87	2.67 ± 0.04	4.92 ± 0.31	1.02	149.25 ± 4.49	12.78 ± 0.81	
1% TJPC	69.63 ± 0.46	40.41	2.59 ± 0.09	5.86 ± 0.43	20.32	179 ± 1.18	15.06 ± 1.11	
2% TJPC	67.2 ± 1.04	35.51	2.57 ± 0.07	5.72 ± 0.64	17.45	161.54 ± 2.50	13.75 ± 1.53	

Applied Polymer SCIENCE

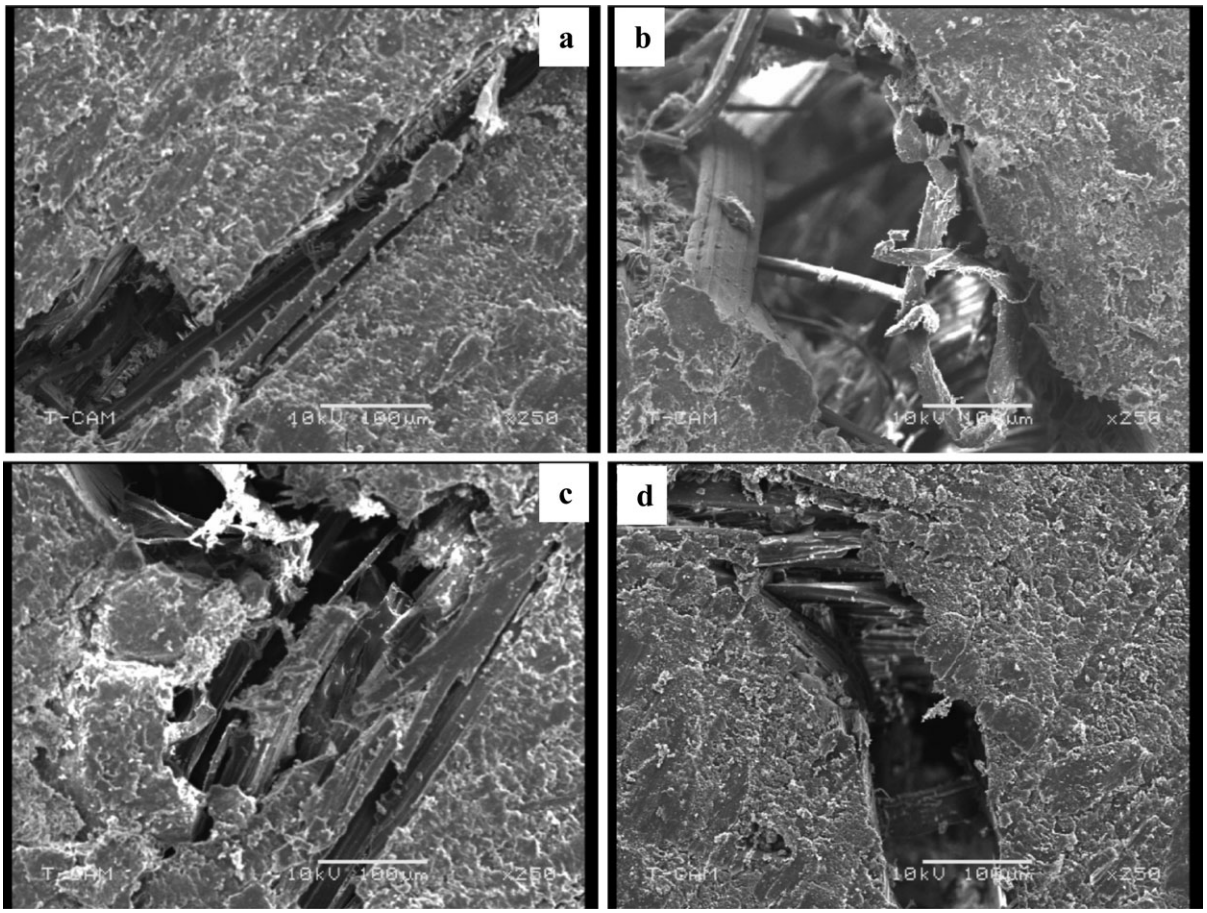

Figure 4. SEM micrographs after flexure test. (a) UTJPC, (b) TJPC, (c) 1% nanoclay TJPC, and (d) 2% nanoclay TJPC.

difference from the statistical viewpoint. The single *P* value was calculated for this purpose. If the *P* value <0.05, the data from different categories can be considered statistically distinct. Otherwise, they are assumed to belong to the same population. The smaller the *P* value is, the more significant the differences are among different categories.[26] In our case, the calculated *P* value for the normalized flexural strength was found to be 0.0001. This very small *P* value (0.0001) substantiates that the addition of a small amount of nanoclay affects the flexural strength of jute fiber reinforced polyester composites in a statistically significant way.

Interlaminar Shear Strength (ILSS) Test Results. Table III shows ILSS test results of jute polyester composites. About 45% improvement in the ILSS was observed in the TJPC compared with the UTJPC and about 49% higher improvement in the 1% nanoclay infused TJPC compared with the UTJPC. The normalized ILSS strengths with standard deviations are also presented in Table III. The normalized strength of the TJPC as well as nanoclay-loaded TJPC showed also an increase in apparent ILSS compared to that of the UTJPC demonstrating better strength in the nanoclay-loaded composite. The *P* value was calculated for ANOVA analysis. The small *P* value (0.0003) confirmed the positive effect of nanoclay addition.

Quasi-Static Compression Test Results. Compression properties of jute polyester composites are shown in Figure 5 and Table IV. The highest compression strength was observed in the 1% nanoclay infused TJPC. However, the highest compression modulus was observed in the 2% nanoclay infused TJPC due to the stiffened matrix. Higher values of normalized compressive strength and modulus of the TJPC and nanoclay-loaded TJPC

Table III. Interlaminar Shear Strength (ILSS) Results of Jute Polyester Composites

	ILSS (MPa)	Standard deviation (MPa)	Change in ILSS (%)	Normalized ILSS (MPa/V_f)	*P*-value from ANOVA test (ILSS)
UTJPC	5.84	0.27	0	13.01 ± 0.60	0.0003
TJPC	8.26	0.75	45.4	21.45 ± 1.95	
1% TJPC	8.49	0.89	49.4	21.83 ± 2.29	
2% TJPC	6.18	0.41	8.8	14.86 ± 0.99	

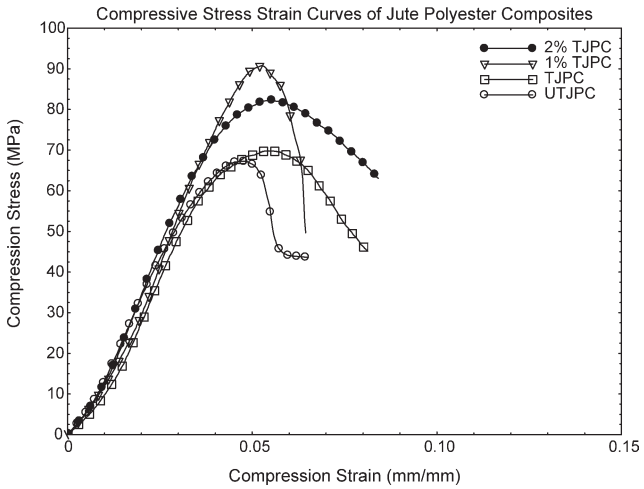

Figure 5. Compression stress–strain curves of jute polyester composites.

were obtained compared to those of the UTJPC (Table IV). The small single *P* value (0.0001) derived from the ANOVA test for the compressive strength confirmed that the addition of nanoclay affected the compressive properties of jute fiber reinforced composites in a statistically significant way. Optical micrographs of the jute-polyester composites (JPC) after compression tests are shown in Figure 6.

Fourier Transform-Infrared (FTIR) Results. Figure 7 shows the FT-IR transmission spectra of neat, 1 wt %, and 2wt % nanoclay loaded polyester. The band at 3448 cm^{-1} is related to stretching vibrations of O-H groups. In neat polyester, there are unsaturated C=H stretching vibration at about 2950 cm^{-1} wave number. This vibration peak shifted to lower wave number in nanoclay loaded polyester for the interaction between polyester resin and nanoclay. In the spectrum of neat polyester, a very intensive band was observed at 1728 cm^{-1} due to stretching vibrations of C=O group. This intensive band disappeared in nanoclay infused polyester. It might have happened due to the reaction with nanoclay. Weak bands near 1500 cm^{-1}observed in the spectrum of polyester resin can be assigned to aromatic ring of polyester.[48]

Water Absorption Results. The water absorption results of jute polyester composites are shown in Table V. Composite panels were allowed to cure at least 24 h at room temperature and then postcured at 110°C for 3 h. Successive room temperature curing and postcuring complete the crosslinking reaction and result in complete curing of the specimens. After postcuring, the specimens were prepared for the tests. Before water absorption tests, the samples were dried in an oven at 105°C for 2 h to remove any residual moisture from the samples. After postcuring at 110°C for 3 h, additional 2-h drying is not expected to induce reaction of the residual reactivity. However, residual reactivity tests on the cured resin were not done in this study. Untreated fiber reinforced composites showed the highest percentage of water absorption among jute polyester composites.

DISCUSSION

From the fiber volume fraction analysis, a higher percentage of voids were found in the UTJPC compared with the TJPC. This

Table IV. Compression Test Results of Jute Polyester Composites

	Compression strength (MPa)	Change in strength (%)	Strain at maximum stress (mm/mm)	Modulus (GPa)	Change in modulus (%)	Normalized strength (MPa/V_f)	Normalized modulus (GPa/V_f)	*P*-value from ANOVA test (strength)
UTJPC	67.42 ± 2.41	0	0.046 ± 0.003	2.06 ± 0.24	0	150.16 ± 5.37	4.59 ± 0.54	0.0001
TJPC	71.38 ± 1.88	5.87	0.055 ± 0.004	2.11 ± 0.11	2.66	185.40 ± 4.88	5.49 ± 0.29	
1% TJPC	90.41 ± 2.35	34.09	0.054 ± 0.004	2.28 ± 0.26	10.82	232.42 ± 6.04	5.87 ± 0.67	
2% TJPC	80.62 ± 1.48	19.57	0.056 ± 0.008	2.56 ± 0.48	24.46	193.8 ± 3.56	6.16 ± 1.15	

Applied Polymer SCIENCE

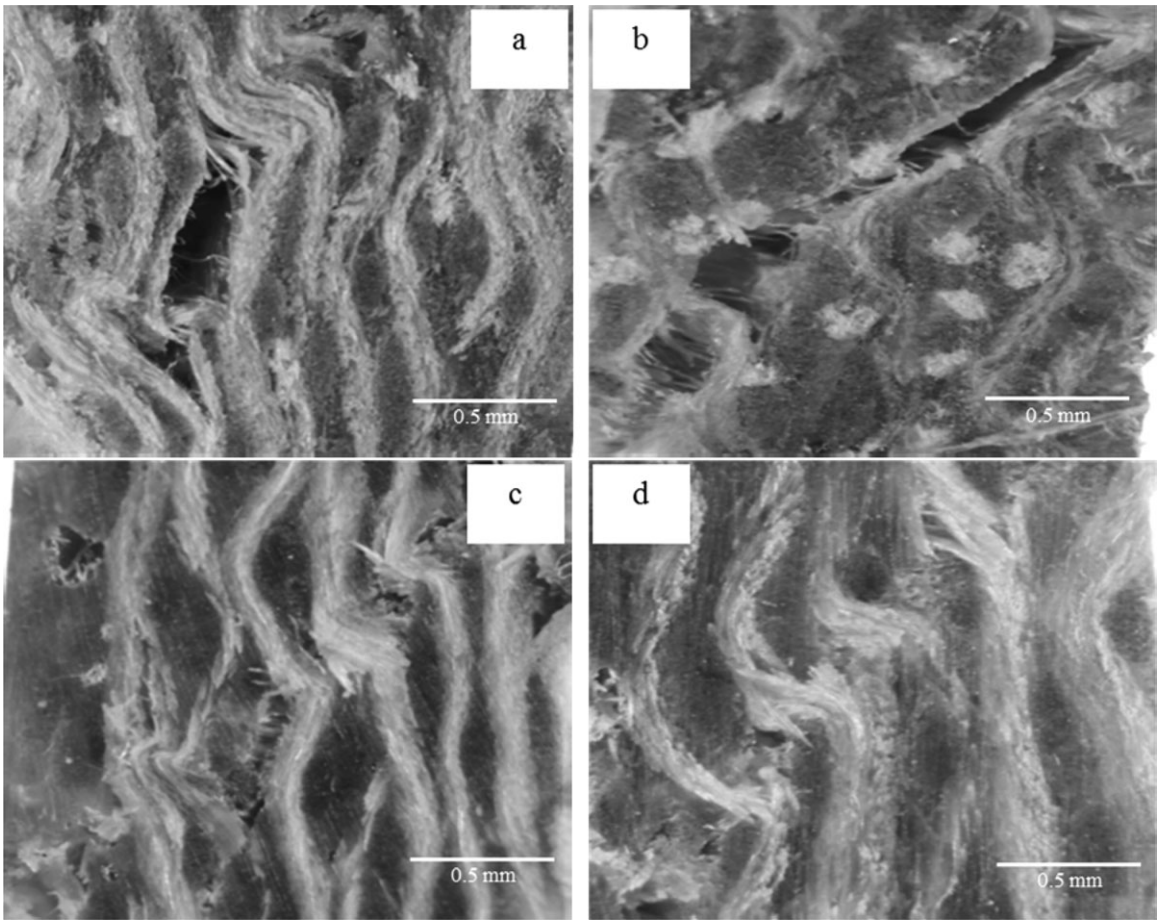

Figure 6. Optical micrographs after compression test. (a) UTJPC, (b) TJPC, (c) 1% nanoclay TJPC, (d) 2% nanoclay TJPC.

was expected due to the lack of proper interaction between the fibers and matrix. A lower void content was found in the nanoclay infused TJPC samples. Nanoclay reduces void spaces in the composites. The highest fiber volume fraction in the UTJC is attributed to improper fiber wetting or lower resin soaking.

This filtration effect generally occurs in nanoparticle infused composites fabricated by the VARTM process due to the filtering role of the fabrics.[26,36,43] This filtering effect results in an inhomogeneous microstructure in the nanophased composites. Nanoclay loading increases the viscosity of the resin mixture and reduces the flow into the fabric significantly. Thus, the driving pressure becomes insufficient to overcome this filtering and viscous resistance effect. As a result, the nanoparticles become less dense in the downstream of the mold and sometimes nanoparticle-loaded resin fails to penetrate the fabric layers at a higher concentration.[26,36] In this study, biaxial hessian jute fabric was used as fiber, which has larger gap and porosity compared with synthetic fibers to pass nanoclay-loaded resin without too much filtering effect. During fabrication, the warp and weft fibers were aligned on the mold in such a way that each layer maintains the same direction of reinforcement. In our case, nonporous Teflon, a distribution mesh, and porous Teflon were placed on the mold. The fabric was placed on top of the porous Teflon. After laying up the required number of layers, another porous Teflon and distribution mesh were placed over the preform. Resin supply and exhaust tubes were connected to a spiral tube along with the distribution mesh that

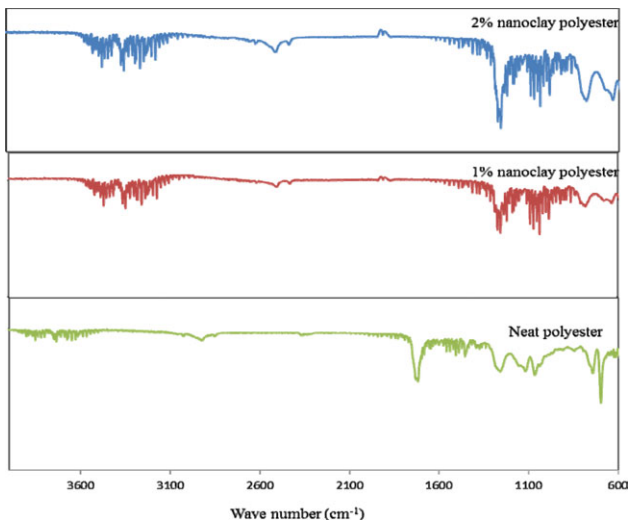

Figure 7. FT-IR transmission spectra of neat and nanoclay loaded polyester. [Color figure can be viewed in the online issue, which is available at wileyonlinelibrary.com.]

Table V. Water Absorption of Jute Polyester Composites After 24 h

	Water gain after 24 h (%)	Standard deviation (%)
UTJPC	6.83	0.93
TJPC	4.54	0.53
1% TJPC	4.42	0.55
2% TJPC	4.14	0.61

lies on top and bottom of the preforms. This facilitates easy flow of resin over the top and through the thickness of the laminate when vacuum was applied. This distribution-media-assisted VARTM process might also reduce the filtration effect.[43,49]The variation in storage modulus, loss modulus, and glass transition temperature (T_g) of the jute polyester composite with surface treatment and nanoclay loading was studied by dynamic mechanical analysis. Storage modulus is related to the cross linking density in the specimens. Crosslinking was initiated by adding 0.7 wt % of MEKP as an initiator to the resin-clay mixture at room temperature just before infusing it into the laminates. The organically modified nanoclay facilitated the nanocomposite formation by increasing the gallery spacing and creating a more hydrophobic environment for the polyester resin and curing agent.[50] This involves swelling the organophilic clay with polyester followed by a crosslinking reaction. During swelling, the monomer diffuses from the bulk monomer into the galleries between the nanoclay layers. Additional reactions might have taken place due to the amine present in the surfactant in the organoclay by enhancing the polymerization rate.[51] Uhl et al. showed that the presence of nanoclay facilitates increased crosslinking reaction in a polymeric composite that, in turn, increased the crosslinking density.[52] They also concluded that nanoclay might be acting as a crosslink and that physical aggregation of polymer chains onto the surface of nanoparticles results in a rise in the effective degree of crosslinking. The storage modulus increased slightly with clay loading in the rubbery plateau region. The increased modulus in the rubbery region is an indication of the clay particles' action as pseudo crosslinks in the polyester resin, which in turn, provide better interfacial bonding between the polyester resin and clay.[36] In our DMA study, the 2 wt % nanoclay-infused composite exhibited the highest storage modulus. This is attributed to the stiffened matrix and confinement of molecular chain movement by uniform nanoclay dispersion. In 1 wt % nanoclay-loaded samples, nanoclays were too dispersed to effectively confine the molecular chain movement in the composites. This leads to a slightly lower value of the storage modulus of these samples.[50] UTJPC and TJPC showed average T_g about 115°C and 116°C, respectively. 2 wt % nanoclay infused TJPC showed T_g about 3°C higher compared with UTJPC. T_g depends on crosslinking density and crosslinking density is related to the dispersion and amount of nanoparticles in the composites. The nanoclay-infused composites exhibited only a small increase in the T_g values. This is an indication of a small degree of improvement in the crosslinking density. The strong adhesion between the resin and clays restricts the motion near the organic–inorganic interface, which may shorten the polymer chain causing an increase in the thermal stability. Thus, the presence of nanoclay enhances the T_g values in the nanoclay-infused specimens as polymer chain confinement effect is increased.[53] However, 1 wt % nanoclays were dispersed and 2 wt % nanoclays were agglomerated resulting in insignificant improvement in the T_g values in our study. Thus, overall enhancement on thermal properties is due to the presence of nanoclay, which acted as barriers to the molecular movement and hindered the diffusion of volatile decomposition products out from the nanocomposites.

Flexure tests were performed to evaluate the bulk stiffness and strength of jute polyester composites. Surface treatment of fibers leads to a better interaction between fiber and matrix and results in a better flexural strength. This was attributed to the dissolution of hemicellulose, fibrillation and enhancement in the crystallinity of the fibers.[24.] Surface treatment also resulted in more cellulose available in the fibers to withstand bending force of the composites. Moreover, the presence of layers of clay in the interfacial region of fiber and matrix further improves interfacial properties of the composites.[54] In essence, nanoclay/jute fiber/polyester ternary cohesive microstructures may restrict the mobility of the matrix in the interface between the fiber and matrix or between the clay and matrix in the composites, allowing better stress transfer to the fibers inside the laminated composites. This would lead to an increased modulus under low strain.[36] Hence, samples with 1 wt % nanoclay showed better mechanical properties compared with the 2 wt % nanoclay-loaded samples due to the uniform dispersion of clay particles into the composite system. Two SEM micrographs (different magnification) in Figure 8(b) demonstrates that nanoclays are well separated and uniformly embedded in the resin system for the 1 wt % sample, which facilitate a better interaction between the fiber and matrix because of the high specific surface area and aspect ratio of the clay. In turn, the better interaction between the fiber and matrix aids to an efficient stress transfers from the continuous polymer matrix to the dispersed fiber reinforcement through the mechanical interlocking of the nanoclay with the fibers. On the other hand, as nanoclay loading increases to 2 wt %, nanoclays start to agglomerate. Two SEM micrographs (different magnification) in Figure 8(c) provide the evidence. These agglomerations produce stress concentration which acts as crack initiation sites by splitting up easily under applied load.

On the other hand, virgin polyester resin showed smooth fracture surface, whereas nanoclay-loaded polyester resin showed rougher fracture surface (Figure 8). A smooth fracture surface is attributed to the brittle failure and a rougher fracture surface is attributed to a tougher material[35] that requires higher energy to break the sample. Nanoparticles deviate the crack propagation front around them, thus creating new surfaces. These surfaces, in turn, produce rougher surfaces in the nanocomposite. Hence, nanoclays dispersed in the polyester matrix act as a barrier and prevent large-scale fragmentation of the matrix. It has been reported that even at low concentration of nanoparticles the fracture energy of polyester nanocomposites could be doubled.[34] However, optimal loading and uniform dispersion of nanoparticles in matrix are the key parameters to promote better nanoparticles-matrix interface properties to reach an efficient load

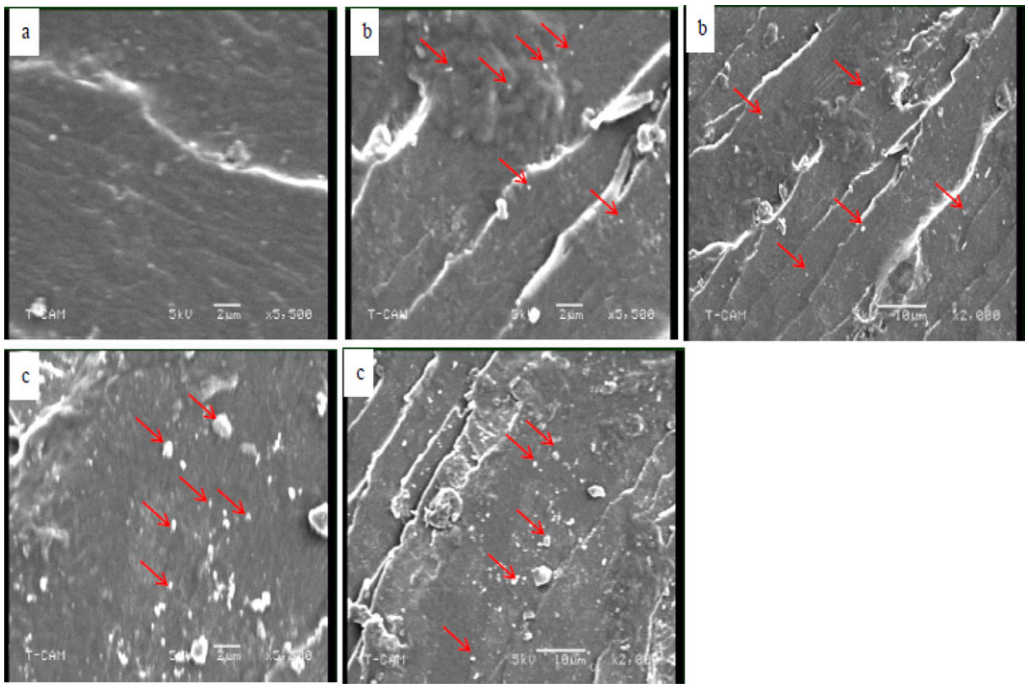

Figure 8. SEM micrographs of (a) neat polyester, (b) 1 wt % nanoclay-loaded polyester (×5500 and ×2000), and (c) 2 wt % nanoclay-loaded polyester (×5500 and ×2000). [Color figure can be viewed in the online issue, which is available at wileyonlinelibrary.com.]

transfer between the two constituents of the nanocomposite.[55–57] At a higher loading of nanoclay, the free volume allowed for nanoclay particles to move around decreases. The modulus, a low deformation property, was not affected by the high stress concentrations caused by the agglomerated particles. However, the strength was reduced by initiating premature failure in the matrix even before shear yielding started.[55] This explains the decrease in the flexural properties in the 2 wt % nanoclay-loaded composites. In case of TJPC, interfacial debonding occurred first followed by the fiber breakage. Nanoclay infused TJPC also showed interfacial debonding followed by fiber breakage. TJPC sample with 1 wt % nanoclay showed a better bonding between the fiber and matrix, which also resulted in the better flexural properties. A higher percentage nanoclay may agglomerate and act as flaws and crack initiation sites in composites.[50] It also helps in the debonding.

In SBS test, the maximum shear stress occurs at the neutral plane where normal stresses are zero. SBS test is the resultant of fiber rupture, microbuckling, and interlaminar shear cracking.[58] Interlaminar shear failure may not occur at the mid plane and it is difficult to assure pure shear failure during the ILSS test.[59] Interlaminar shear properties are very important in composite materials, because failure of composites sometimes occurs in the interfacial region. Surface treatment results in a better interfacial bonding between fiber and matrix and nanoclay prevents the crack generation and crack propagation into the composites. However, 2% nanoclay addition lowered the ILSS in our samples due to two processing limitations: (1) agglomeration of nanoclay [Figure 8(c)] in the interfacial region which helps debond the fiber from the matrix easily and (2) the filtering effect might limit the complete wetting out of all fabric layers as well as the uniform dispersion of 2 wt % nanoclay throughout the composite.[26,36,43,60] Standard deviation of each category of tests ranged from 0.6 to 2.29%. The small standard deviation values indicate that all samples failed by interlaminar shear.[61]

Surface treated fibers results in a better interfacial bonding between the fiber and matrix, thus a significant improvement was observed in the compressive strength and modulus in the TJPC compared with the UTJPC. Moreover, the presence of nanoclay in the polyester matrix strengthens and stiffens the surrounding matrix. This strengthened and stiffened matrix effectively increases the compressive strength of the composite. Specimens with 2% nanoclay showed lower compressive strength due to improper mixing at a higher nanoclay loading.[21] The increase in compression modulus in nanoclay infused samples can be attributed to the decrease in molecular movement with the nanoclay loading and presence of stiffer and stronger matrix in the composite. Higher values of normalized compressive strength and modulus of the TJPC and nanoclay-loaded TJPC were obtained compared with those of the UTJPC (Table IV). Moreover, nanoclay-loaded samples exhibited the best results. In case of UTJC, failure occurred due to interfacial debonding as well as fiber microbuckling (Figure 6). In TJPC, no debonding was observed due to better interaction between the fiber and matrix. Here failure occurred due to fiber microbuckling and matrix cracking. Similar trends were observed in the nanoclay infused TJPC. Here the cracks did not propagate linearly due to the presence of nanoclay, which resulted in better compressive properties.

Untreated fiber reinforced composites showed the highest percentage of water absorption among jute polyester composites.

The water absorption occurs due to capillary action of the fibers.[62] Untreated fiber reinforced composites had more microcracks compared with treated fiber reinforced composites. Water molecules are absorbed by the fiber through microcracks. The capillary mechanism is involved in the transportation of the water molecules through the composites. Treated fiber reinforced and nanoclay infused samples had lower microcracks, resulting in lower water absorption compared with untreated fiber reinforced composites. On the other hand, clay sheets are naturally impermeable. They increase the barriers properties of polymers by creating a maze or tortuous path that retards the diffusion of water/gas molecules through the polymer matrix into the composites. Hence, nanoclay-loaded treated jute fiber reinforced polyester composites demonstrated the lowest water absorption in this study.

In nanoclay-loaded composites, the nanoclay will have at least one dimension in the nanoscale and its uniform dispersion within the polymer matrix will facilitate the tremendous interfacial contacts between the polymer and inorganic/organic filler. This adequate polymer-clay interfacial interaction allows the nanoclay to carry the major portion of applied load to the polymer matrix and polymer matrix to the fiber by bridging effect under stress conditions.[63,64] Thus, any enhancement in the polymer-clay interfacial contact leads to the better stress transfer in the nanoclay incorporated fiber reinforced polymer nanocomposite. In essence, a greater adhesion between the matrix and inclusion results in less debonding during the application of load. As a result, the elastic modulus and strength are found to be improved. Since the organoclay is hydrophobic due to the presence of organofunctional vinyl group, it interacts strongly with the polymer matrix. That is also evident from the FT-IR study. This results in a greater adhesion between the matrix and the filler at the interface of the composite.[54] This improved interface is developed only when the amount of nanoclay ranging from 0 to 2 wt % is intercalated and/or exfoliated into the polymeric matrix using the combination of mechanical and sonication mixing methods. Addition of nanoclay above this critical level adversely affects the final properties of the composite produced by the VARTM process due to increase in the bulk viscosity of the polymer. The increased viscosity will require excessive injection pressure for molded composite.

In higher clay loadings, breaking down clay clusters, removing micro-air pockets, and achieving full dispersion might not be possible by mechanical mixing or sonication, even for low viscosity matrices commonly used in liquid composite molding (LCM) processes such as VARTM.[65] Thus, poor dispersion of more than 2 wt % nanoclay is thought to lead to poor interface which will result in poor mechanical properties. Moreover, it was observed in our study that the viscosity of the matrix increased as clay content increased, which allowed small air bubbles to be trapped in the resin during mixing process forming tiny voids in the sample. This in turn resulted in sample failure at relatively low stress. On the other hand, at a lower loading of nanoclay, the probability of the formation of microvoids is less, and the dispersion is more uniform which both lead to strength improvement.[66] In essence, at high concentration of clay, nanoclay poorly dispersed inside the matrix forming platelet agglomerations which act as stress concentrators which in turn cause reduction in properties of the composite. There are possible three scenarios thought to be responsible for worse wetting of the fiber that results in poor properties in the fiber reinforced polymer composites due to increased viscosity resulting in at a higher clay loading: (1) the polymer is unable to intercalate within the clay layers during mixing and the clay is dispersed as aggregates or particles with layers stacked together within the polymer matrix. Infusing of this polyester-clay mixture into the jute fiber using the VARTM process will produce a phase separated composites. The properties of phase separated jute/polyester-clay composites will be in the range of traditional microcomposites; (2) void occurrence is observed to increase considerably with increasing nanoclay content from 2.1% in the composite without nanoclay to 5.1% and 8.3% in the composites molded with 5 and 10 wt % nanoclay, respectively. However, the composite with 2 wt % nanoclay yields the lowest void content of 0.7%. On the other hand, combination of mechanical and sonication mixing, and degassing led to almost void free resins containing 0 and 2 wt % clay content.[65]

There are three possible void locations in the molded parts. First location is areas primarily composed of reinforcing fibers. Voids in this region are intratow voids situated within fiber bundles (perform voids). Second location is areas rich in matrix without fibers. Voids in this location are totally surrounded by the clay-epoxy blend (matrix voids). The third location is the transitional areas between these two locations. Voids situated in this location are always positioned adjacent to, but not within fiber bundles (transition voids). At higher resin front velocities, resin flow outside fiber tows in much faster than inside, and voids (intratow voids) are primarily formed inside the fiber bundles. Increased viscosity of the resin due to higher clay loading causes to infuse the resin into the fiber at a very slower rate. This leads to capillary flow inside fiber tows and voids (intertow) are formed outside of the fiber bundles. On the other hand, void might be augmented in the resin due to the presence of air pockets inside larger clay clusters due to a higher resin viscosity. Thus, presence of voids outside of the fiber and in the resin will create a weaker interface and ultimately will yield poor properties in the composite; and (3) higher viscosity may cause lesser increase in the properties of composites with the formation of agglomerates of nanoclays on fiber surface, which affects the effective bond between the fiber and the matrix.[67] This phenomenon is explained based on the monomolecular layer (MML) formation theory in case of micron sized LaCl3 particles. When the MML is formed, the two corresponding surfaces adheres each other efficiently through the chemical bridge with MML. When agglomerates of nanoclays exist on the interface, instead of MML, multimolecular layers (MTML) are formed and adhesion amongst these is based on weak Van der Waals force resulting in less stronger composite.[68]

CONCLUSIONS

Alkali-treated jute fiber reinforced composites showed better thermomechanical properties compared with UTJPC for the better adhesion between fiber and matrix. Microstructural

studies showed superior bonding between the fiber and matrix in the nanoclay infused composite and TJPC. For better adhesion and water barrier properties of nanoclay, TJPC and nanoclay infused TJPC showed lower water absorption. The maximum flexural, ILSS, and compression properties were observed in the 1% nanoclay-loaded TJPC. Composites with 2 wt % nanoclay loading showed declining trends in the properties except DMA results. FT-IR study showed strong interaction between polyester matrix and organoclay. Low P values (<0.05) calculated by ANOVA tests in all cases confirmed that the addition of nanoclay affected the properties of jute fiber reinforced composites in a statistically significant way. Overall this work showed that alkali treatment and nanoclay loading can be easily used to modify the properties of traditional natural fiber reinforced composite materials for structural applications.

ACKNOWLEDGMENTS

The authors acknowledge the financial support of NSF-EPSCoR grant no. EPS-0814103 and NSF-RISE grant no. HRD-0833158 for this research work.

REFERENCES

1. Doan, T.; Gao, S.; Mader, E. *Compos. Sci. Technol.* **2006**, *66*, 952.
2. Gowda, T. M.; Naidu, A. C. B.; Chhaya, R. *Compos. A* **1999**, *30*, 277.
3. Zini, E.; Focarete, M. L.; Noda, I.; Scandola, M. *Compos. Sci. Technol.* **2007**, *67*, 2085.
4. Ahmed, K. S.; Vijayarangan, S. *J. Mater. Process. Technol.* **2008**, *207*, 330.
5. Dweib, M. A.; Hu, B.; O'Donnell, A.; Shenton, H. W.; Woll, R. P. *Compos. Struct.* **2004**, *63*, 147.
6. Bevitori, A. B.; Da Silva, I. L. A.; Lopes, F. P. D.; Monterio, S. N. *Rev. Matér.* **2010**, *15*, 125.
7. Gassan, J.; Bledzki, A. K. *Compos. Sci. Technol.* **1999**, *59*, 1303.
8. Ray, D.; Sarkar, B. K.; Das, S.; Rana, A. K. *Compos. Sci. Technol.* **2002**, *62*, 911.
9. Mohanty, A. K.; Khan, M. A.; Hinrichsen, G. *Compos. Sci. Technol.* **2000**, *60*, 1115.
10. Sandler, J.; Werner, P.; Shaffer, M. S. P.; Denchuk, V.; Altstadt, V.; Windle, A. H. *Compos. A* **2002**, *33*, 1033.
11. Bruzaud, S.; Bourmaud, A. *Polym. Test.* **2007**, *26*, 652.
12. Yasmin, A.; Abot, J. L.; Daniel, I. M. *Scr. Mater.* **2003**, *49*, 81.
13. Giannelis, E. P. *Appl. Organomet. Chem.* **1998**, *12*, 675.
14. Vaia, R. A.; Jandt, K. D.; Kramer, E. J.; Giannelis, E. P. *Chem. Mater.* **1996**, *8*, 2628.
15. Aranda, P.; Ruiz-Hitzky, E. *Chem. Mater.* **1992**, *4*, 1395.
16. Greenland, D. J. *J. Colloid. Sci.* **1963**, *18*, 647.
17. Dash, B. N.; Rana, A. K.; Mishra, H. K.; Ncyak, S. K.; Mishra, S. C.; Tripathy, S. S. *Polym. Compos.* **1999**, *20*, 62.
18. Saha, A. K.; Das, S.; Bhatta, D.; Mitra, B.C. *Appl. Polym. Sci.* **1999**, *71*, 1505.
19. Akil, H. M.; Cheng, L. W.; Ishak, Z. A. M.; Bakar, A. A.; Rahman, M. A. A. *Compos. Sci. Technol.* **2009**, *69*:1942.
20. Ahmed, S. K.; Vijararnagan, S.; Naidu, A. C. B. *Mater. Des.* **2007**, *28*, 2287.
21. Ahmed, S. K.; Vijararnagan, S. J. *Mater. Process. Technol.* **2008**, *207*, 330.
22. de Albuquerque, A. C.; Kuruvilla, J.; Laura, H.; Morais, A. J. R. *Compos. Sci. Technol.* **2000**, *60*, 833.
23. Jiang, L.; Morelius, E.; Zhang, J.; Wolcott, M.; Holbery, J. *J. Compos. Mater.* **2008**, *42*, 2629.
24. Ray, D.; Sarkar, B. K.; Rana, A. K.; Bose, N. R. *Compos. A* **2001**, *32*, 119.
25. Hwang, B.; Kim, B.; Lee, J.; Byun, J.; Park, J. In Proceedings of 16th international conference on composite materials, Kyoto, Japan, July 8–13, **2007**.
26. Fan, Z.; Santare, M.; Advani, S. *Compos. A* **2008**, *39*, 540.
27. Post, N. L.; Riebel, F.; Keller, T.; Case, S. W.; Lesko, J. J. *J. Compos. Mater.* **2009**, *43*, 75.
28. Abot, J. L.; Yasmin, A.; Daniel, I. M. *J. Reinf. Plast. Compos.* **2005**, *24*, 195.
29. Assarar, M.; Scida, D.; Mahi, A. E.; Poilane, C.; Ayad, R. *Mater. Des.* **2011**, *32*, 788.
30. Jawaid, M.; Khalil, H. P. S. A. *Carbon Polym.* **2011**, *86*, 1.
31. Fraga, A. N.; Frullloni, E.; de la Osa, O.Kenny, J. M.; Va'zquez, A. *Polym. Test.* **2006**, *25*, 181.
32. Vilay, V.; Mariatti, M.; Taib, R. M.; Todo, M. *Compos. Sci. Technol.* **2008**, *68*, 631.
33. Yasmin, A.; Abot, J. L.; Daniel, I. M. *Mater. Res. Soc. Symp. Proc.* **2003**, *740*:75.
34. Jawahar, P.; Gnanamoorthy, R.; Balasubramanian, M. *Wear* **2006**, *261*, 835.
35. Haq, M.; Burgueno, R.; Mohanty, A. K.; Misra, M. *Compos. A* **2009**, *40*, 394.
36. Lin, L. Y.; Lee, J. H.; Hong, C. E.; Yoo, G. H.; Advani, S. G. *Compos. Sci. Technol.* **2006**, *66*, 2116.
37. Seki, Y. *Mater. Sci. Eng. A* **2009**, *508*, 247.
38. Acha, B. A.; Marcovich, N. E.; Reboredo, M. M. *Appl. Polym. Sci.* **2005**, *98*, 639.
39. Xi, Y.; Frost, R. L.; He, H.; Kloprogge, T.; Bostrom, T. *Langmuir.* **2005**, *21*, 8675.
40. Valadez-Gonzalez, A.; Cervantes-Uc, J. M.; Olayo, R.; Herrera-Franco, P. J. *Compos. B* **1999**, *30*, 309.
41. Vilaseca, F.; Mendez, J. A.; Pelach, A.; Llop, M.; Canigueral, N.; Girones, J.; Turon, X.; Mutje, P. *Process. Biochem.* **2007**, *42*, 329.
42. Eskin, G. I. *Ultrason. Sonochem.* **2001**, *8*, 319.
43. Sadeghian, R.; Gangireddy, S.; Minaie, B.; Hsiao, K. *Compos. A* **2006**, *37*, 1787.
44. Hossain, M. K.; Dewan, M. W.; Hosur, M.; Jeelani, S. *Compos. B* **2011**, *42*, 1701.
45. Annual Book of ASTM Standards, D 4065-01, Standard Practice for Determining and Reporting Dynamic Mechanical Properties of Plastics, ASTM International: West Conshohocken, PA, **2002**.

46. Jawarid, M.; Khalil, A.; Bakar, A.; Khanam, N. *Mater. Des.* **2011**, *32*, 1014.
47. Rutherford, A. Introducing ANOVA and ANCOVA: A GLM Approach (Introducing Statistical Methods Series); Sage Publications Ltd.: London, **2001**.
48. Cecen, V.; Seki, Y.; Sarikanat, M.; Tavman, I. H. *J. Appl. Polym. Sci.* **2008**, *108*, 2163.
49. Chowdhury, F. H.; Hosur, M. V.; Jeelani, S. *Mater. Sci. Eng. A* **2006**, *421*, 298.
50. Timmerman, J. F.; Hayes, B. S.; Seferis, J. C. *Compos. Sci. Technol.* **2002**, *62*, 1249.
51. Xu, Y.; Hoa, S. V. *Compos. Sci. Technol.* **2008**, *68*, 854.
52. Uhl, F. M.; Davuluri, S. P.; Wong, S.; Webster, D. C. *Polymer* **2004**, *45*, 6175.
53. Pramoda, K. P.; Linh, N. T. T.; Tang, P. S.; Tjiu, W. C.; Goh, S. H.; He, C. B. *Compos. Sci. Technol.* **2010**, *70*, 578.
54. Bozkurt, E.; Kaya, E.; Tanoglu, M. *Comp. Sci. Technol.* **2007**, *67*, 3394.
55. Zhou, Y., Pervin, F.; Jeelani, S.; Mallick, P. K. *J. Mater. Process. Technol.* **2008**, *198*, 445.
56. Prolongo, S. G.; Burón, M.; Gude, M. R.; Chaos-Morán, R.; Campo, M.; Ureña, A. *Compos. Sci. Technol.* **2008**, *68*, 2722.
57. Ghosh, R.; Reena, G.; Khirshan, A. R.; Raju, B. L. *Int. J. Adv. Eng. Sci. Technol.* **2011**, *4*, 89.
58. Subramaniyan, A. K.; Sun, C. T. *Compos A* **2006**, *37*, 2257.
59. Mallick, P. K. Fiber Reinforced Composite Materials, Manufacturing and Design, 2nd ed.; Marcel Dekker, Inc.: New York, **1993**; p 243.
60. Green, K. J.; Dean, D. R.; Vaidya, U. K.; Nyairo, E. *Compos. A* **2009**, *40*, 1470.
61. Rodriguez, A. J.; Guzman, M. E.; Lim, C. S.; Minaie, B. *Carbon* **2011**, *49*, 937.
62. Dhakal, H. N.; Zhang, Z. Y.; Richardson, M. O. W. *Compos. Sci. Technol.* **2007**, *67*, 1674.
63. Tortora, M.; Vittoria, V.; Galli, G.; Ritrovati, S.; Chiellini, E. *Macromol. Mater. Eng.* **2002**, *287*, 243.
64. Gorrasi, G.; Tortora, M.; Vittoria, V.; Pollet, E.; Lepoittevin, B.; Alexandre, M. *Polymer* **2003**, *44*, 2271.
65. Hamidi, Y. K.; Aktas, L.; Altan, M. C. *J. Thermoplast. Compos. Mater.* **2008**, *21*, 141.
66. Alamri, H.; Low, I. M.; Alothman, Z. *Compos. B* **2012**, *43*, 2762–2771.
67. Li, J.; Cheng, X. H. *Tribol. Lett.* **2007**, *25*, 207–214.
68. Shang-guan, Q. Q.; Cheng, X. H. *Wear* **2007**, *262*, 1419.